

ER-localized bestrophin 1 activates Ca^{2+} -dependent ion channels TMEM16A and SK4 possibly by acting as a counterion channel

René Barro-Soria · Fadi Aldehni · Joana Almaça ·
Ralph Witzgall · Rainer Schreiber · Karl Kunzelmann

Received: 19 June 2009 / Revised: 29 September 2009 / Accepted: 30 September 2009 / Published online: 13 October 2009
© Springer-Verlag 2009

Abstract Bestrophins form Ca^{2+} -activated Cl^- channels and regulate intracellular Ca^{2+} signaling. We demonstrate that bestrophin 1 is localized in the endoplasmic reticulum (ER), where it interacts with stromal interacting molecule 1, the ER- Ca^{2+} sensor. Intracellular Ca^{2+} transients elicited by stimulation of purinergic P2Y_2 receptors in HEK293 cells were augmented by hBest1. The p21-activated protein kinase Pak2 was found to phosphorylate hBest1, thereby enhancing Ca^{2+} signaling and activation of Ca^{2+} -dependent Cl^- (TMEM16A) and K^+ (SK4) channels. Lack of bestrophin 1 expression in respiratory epithelial cells of mBest1 knockout mice caused expansion of ER cisterns and induced Ca^{2+} deposits. hBest1 is, therefore, important for Ca^{2+} handling of the ER store and may resemble the long-suspected counterion channel to balance transient membrane potentials occurring through inositol triphosphate (IP_3)-induced Ca^{2+} release and store refill. Thus, bestrophin 1 regulates compartmentalized Ca^{2+} signaling that plays an essential role in Best macular dystrophy, inflammatory diseases such as cystic fibrosis, as well as proliferation.

Electronic supplementary material The online version of this article (doi:10.1007/s00424-009-0745-0) contains supplementary material, which is available to authorized users.

René Barro-Soria and Fadi Aldehni contributed equally to the present study.

R. Barro-Soria · F. Aldehni · J. Almaça · R. Schreiber ·
K. Kunzelmann (✉)
Institut für Physiologie, Universität Regensburg,
Universitätsstraße 31,
93053 Regensburg, Germany
e-mail: Karl.Kunzelmann@vkl.uni-regensburg.de

R. Witzgall
Institut für Anatomie, Universität Regensburg,
Universitätsstraße 31,
93053 Regensburg, Germany

Keywords Bestrophin · Ca^{2+} -activated Cl^- currents · CaCC · Ca^{2+} -activated K^+ currents · SK4 · TMEM16A · Pak2 · Purinergic receptors · Endoplasmic reticulum · ER · Ca^{2+} store

Abbreviations

hBest1	human bestrophin 1
CaCC	Ca^{2+} -activated Cl^- channels
SK4	small conductance calcium-activated potassium channel type 4
TMEM16A	transmembrane protein 16A
ANO1	anoctamin 1
Pak2	p21-activated protein kinase
ER	endoplasmic reticulum
SERCA	sarcoendoplasmic reticulum calcium ATPase
Stim1	stromal interacting molecule 1
DIDS	4,4'-diisothio-cyanostilbene-2,2'-disulfonic acid

Introduction

Mutations in human bestrophin 1 (hBest1) are responsible for early onset of macular degeneration called Best vitelliform macular dystrophy [15]. Bestrophins are also upregulated during inflammation and tissue repair and promote proliferation and development of cancer [1, 37]. Compelling evidence has been provided that bestrophins are Ca^{2+} -activated and DIDS-sensitive Cl^- channels (CaCC) [30, 40], but much controversy exists about the question whether these proteins indeed form apical Cl^- channels in epithelial cells [23]. Although it has been shown that hBest1 enhances Ca^{2+} -dependent Cl^- secretion in epithelial cells and that Ca^{2+} -dependent Cl^- secretion is reduced in

airways of Best1^{-/-} knockout animals [4, 5], the precise role of bestrophin 1 for epithelial CaCC is not clear. Moreover, although overexpressed bestrophin 1 can be detected in cell membranes [15, 28], a large fraction of exogenous and particularly endogenous bestrophin 1 is found in intracellular compartments [1, 23, 26]. hBest1 has also been suggested to control intracellular Ca²⁺ signaling, e.g., by controlling voltage-gated Ca²⁺ channels [33]. Because it is not clear how bestrophin 1 controls Ca²⁺-activated Cl⁻ conductance in epithelial cells, we searched for possible links between cytosolic [Ca²⁺], bestrophin 1, and Ca²⁺-activated Cl⁻ currents. Here, we present evidence that, in both native and overexpressing cells, bestrophin 1 is located primarily in the endoplasmic reticulum (ER), where it controls receptor-mediated Ca²⁺ signals, thereby activating Ca²⁺-dependent ion channels. Our data suggest that bestrophin 1 acts as a counterion channel for Ca²⁺ movement over the ER membrane.

Materials and methods

Cell culture, cDNAs, and transfection Cell lines from human embryonic kidney (HEK-293) and human bronchial epithelium (16HBE14o⁻) were cultured as described elsewhere [5]. Complementary DNA (cDNA) for human bestrophin 1 (kindly provided by Dr. J. Nathans, Johns Hopkins University, Baltimore, USA), hStim1 (OriGene Technologies, Rockville, USA), hIP3R-3 (kindly provided by Dr. H. De Smedt, Leuven, Belgium), hTRPC1 (kindly provided by Dr. L. Birnbaumer, Research Triangle Park, USA), hPak2 (kindly provided by Dr. K. Saksela, Tampere, Finland), TMEM16A (cloned from 16HBE14o⁻ cells by reverse transcription polymerase chain reaction [RT-PCR]), SK4 (kindly provided by Dr. W. J. Joiner, New Haven, USA), and the highly Ca²⁺-sensitive GFP protein, G-CaMP2 (kindly provided by Dr. J. Nakai, Wako City, Saitama, Japan [27]) were cloned into mammalian expression vectors. hBest1 and P2Y₂ receptors were His₆-tagged at the C terminus. Site-specific mutations (hBest1-R218C, hBest1-S358A) were introduced using QuickChangeTM (Stratagene, Heidelberg, Germany). G-CaMP2 fusion protein was generated by PCR. All cDNAs were verified by sequencing. Cells were transfected using standard methods (Lipofectamine, Invitrogen, Karlsruhe, Germany). All experiments were performed 48 h after the transfection.

Immunocytochemistry HEK293 cells and 16HBE cells were grown on glass cover slips and washed three times in phosphate-buffered saline (PBS). Cells were fixed with methanol at -20°C for 5 min or with 4% paraformaldehyde and 0.2 M picric acid in PBS for 10 min and incubated with primary antibodies at 4°C overnight. Polyclonal hBest1

antibodies were raised against mouse best1 (sequence AESYPYRDEAGTKPVLYE) or the human best1 (sequence KDHMDPYWALENRDEAHS; Davids Biotechnology, Regensburg, Germany). Mouse monoclonal antihuman calreticulin and mouse monoclonal anti-hSTIM1 antibodies were from BD Transduction Laboratories (Heidelberg, Germany). Mouse monoclonal antihuman calnexin was raised against amino acid residues 116–301. For immunofluorescence, cells were incubated with secondary AlexaFluoro 488 goat antirabbit IgG and tetramethylrhodamine goat antimouse IgG (Molecular Probes) for 1 h at room temperature and counterstained with Hoe33342 (Sigma-Aldrich, Taufkirchen, Germany). Immunofluorescence was detected using an Axiovert 200 microscope equipped with an ApoTome and Carl Zeiss AxioVision software (Axiovert 200M, Zeiss, Jena, Germany).

Measurement of the intracellular Ca²⁺ concentration HEK293 cells were loaded either with 5 μM Fura2-AM (to measure global cytosolic Ca²⁺ changes using standard ratiometric techniques) or membrane-bound Fura-piperazine-C₁₂H₂₅ (FFP-18, TEFLabs, Austin, USA) in Ringer solution at 37°C for 2 h (to measure Ca²⁺ signals close to intracellular membranous compartments such as the ER). Fluorescence was detected at 37°C, using an inverted microscope IMT-2 (Olympus, Nürnberg, Germany) and a high speed polychromator system (Visi-Chrome, Puchheim, Germany). FFP-18 was excited at 340/380 nm, and emission was recorded between 470 and 550 nm using a CCD camera (CoolSnap HQ, Visitron). The results were obtained at 340/380 nm fluorescence ratio (after background subtraction). We further measured cytosolic Ca²⁺ in close proximity to the ER store and bestrophin 1. To that end, we fused the Ca²⁺-sensitive protein G-CaMP2 [27] to hBest1 and to mutant hBest1-R218C, respectively. When using hBest1-G-CaMP2 or hBest1-R218C-G-CaMP2, fluorescence was excited at 485 nm and was detected at 520 to 550 nm.

2D electrophoreses and MALDI-TOF analysis Two-dimensional polyacrylamide gel electrophoresis (2D-PAGE) was performed with immobilized pH gradient (IPG) strip gels (Amersham, Germany) after overnight rehydration at room temperature. Isoelectric focusing was carried out with an IPGphor (Amersham Biosciences) for a total of 16 kV h at 20°C. The IPG gel was equilibrated in 3 M urea, 50 mM Tris-HCl pH 8.8, 30% glycerol, 1.0% sodium lauryl sulfate (SDS), and 16 mM dithiothreitol (DTT) for 15 min. Equilibrated IPG gels were placed on the top of the second-dimension 10% SDS gel with embedding agarose, and second-dimension electrophoresis was performed at room temperature for 5 h. Proteins were silver stained, and spots were excised, trypsin-digested, and analyzed by

matrix-assisted laser desorption/ionization–time of flight (MALDI-TOF) and mass spectrometry database comparison (SEQLAB, Goettingen, Germany).

Immunoprecipitation and Western blotting Protein was isolated from transfected HEK293 cells in lysis buffer containing 50 mM Tris–HCl, 150 mM NaCl, 50 mM Tris, 100 mM DTT, 1% NP-40, 0.5% deoxycholate sodium, and 1% protease inhibitor cocktail (Sigma, Germany). Prior to the addition of 1–5 μg of the primary antibody, protein lysates were precleared with protein A/G agarose beads (Pierce, Rockford, USA). Incubation of the precleared protein lysates with primary antibodies was performed overnight at 4°C, and the protein–antibody complex was immobilized with the addition of 25 μl of 50% slurry of protein A/G– or Ni NTA–agarose beads for 1 h at 4°C. The beads were washed three times in lysis buffer, and after the last washing step, beads were boiled in 1 \times Laemmli sample buffer for Western blot analysis or the proteins were dissolved in 8 M urea, 4% CHAPS, 60 mM DTT, 2% Pharmalyte™ 3–10, 0.002% bromophenol blue for 2D-PAGE analysis. For Western blot analysis, the 10% SDS polyacrylamide gel was transferred to a polyvinylidene difluoride membrane (GE Healthcare Europe GmbH, Munich, Germany) using semidry transfer (BioRad, Munich, Germany). Membranes were incubated with first antibodies (dilution from 1:2,000 to 1:5,000) overnight at 4°C. Proteins were visualized using a horseradish peroxidase (HRP)-conjugated secondary antibody (dilution 1:30,000) and ECL Detection Kit (GE Healthcare, Munich, Germany); the protein bands were detected by FujiFilm LAS-3000.

In vitro phosphorylation Human bestrophin C-terminal domains (wild-type and mutant) were expressed in BL21 (DE3) *Escherichia coli* strain from a plasmid encoding 295 fragments from position 291 to 585 with an N-terminal polyhistidine (6 \times His) tag and SUMO in the pETSUMO™ vector (Invitrogen, Carlsbad, USA). Cells were grown to $A_{600}=0.8$ –1 at 37°C and induced with 0.5 mM IPTG for 12–16 h at 16°C. After production in bacteria, the hBest1C regions were purified through a Talon Metal Affinity Resin (Clontech Laboratories, Mountain View, USA), and samples were further concentrated and exchanged into the buffer of interest. Purity of the samples was analyzed by sodium dodecyl sulfate polyacrylamide gel electrophoresis (SDS-PAGE) and Western blotting. The C-terminal of hBest1 was phosphorylated by Pak2 (300 ng) in 20- μl phosphorylation buffer (25 mM Tris–HCl, pH 7.5, 5 mM MgCl₂, 150 mM KCl, 1 mM DTT) containing 125 μM [γ -³²P] ATP 20 μCi at 30°C for 40 min. The reactions were stopped by 1 \times Laemmli SDS sample buffer and used for analysis by 10% SDS-PAGE. The radioactive SDS gels were dried and analyzed by X-ray film.

Patch clamp Cell culture dishes were mounted on the stage of an inverted microscope (IM35, Zeiss) and kept at 37°C. The bath was perfused continuously with Ringer solution at about 10 ml/min. Patch-clamp experiments were performed in the fast whole-cell configuration. Patch pipettes had an input resistance of 2–4 M Ω , when filled with a solution containing (in millimolars) KCl 30, K-gluconate 95, NaH₂PO₄ 1.2, Na₂HPO₄ 4.8, EGTA 1, Ca-gluconate 0.758, MgCl₂ 1.034, D-glucose 5, ATP 3; pH was 7.2 and the Ca²⁺ activity was 0.1 μM . The access conductance was measured continuously and was 60–140 nS. Currents (voltage clamp) and voltages (current clamp) were recorded using a patch-clamp amplifier (EPC 7, List Medical Electronics, Darmstadt, Germany), the LH1600 interface and PULSE software (HEKA, Lambrecht, Germany) as well as Chart software (AD-Instruments, Spechbach, Germany). Data were stored continuously on a computer hard disk and were analyzed using PULSE software. In regular intervals, membrane voltages (V_c) were clamped in steps of 10 mV from –50 to +50 mV relative to resting potential. Membrane conductance G_m was calculated from the measured current (I) and V_c values according to Ohm's law.

In vitro transcription and double-electrode voltage clamp cDNAs encoding SK4, hBest1-R218C, hBest1-S358A, and hBest1-S358E were linearized and in vitro transcribed using the T7, T3, or SP6 promoter and polymerase (Promega, USA). Two milligrams of Pak2 enzyme was injected into *Xenopus* oocytes 30 min before measurements. Isolation and microinjection of oocytes have been described in detail elsewhere [3]. Oocytes were injected with cRNA (10 ng, 47 nl double-distilled water). Water-injected oocytes served as controls. Two to 4 days after injection, oocytes were impaled with two electrodes (Clark Instruments Ltd, Salisbury, UK), which had resistances of <1 M Ω when filled with 2.7 mol/L KCl. Using two bath electrodes and a virtual ground head stage, the voltage drop across R_{serial} was effectively zero. Membrane currents were measured by voltage clamping (oocyte clamp amplifier; Warner Instruments LLC, Hamden, CT, USA) in intervals from –60 to +0 mV (–90 to +30 mV for SK4-expressing oocytes), in steps of 10 mV, each 1 s. The bath was continuously perfused at a rate of 5 ml/min. All experiments were conducted at room temperature (22°C).

Electron microscopy For conventional electron microscopy, adult mice were perfusion-fixed for 3 min through the distal abdominal aorta with 1 \times PBS/2% glutaraldehyde. Tracheas were removed, incubated overnight in fixative, and treated with 1% OsO₄ before being embedded in Epon. After ultrathin sections were stained with uranyl acetate and lead citrate, they were analyzed with a Zeiss EM 902 transmis-

sion electron microscope equipped with a cooled CCD camera (TRS, Moorenweis, Germany).

To visualize increased Ca^{2+} concentrations in intracellular organelles [41], adult mice were perfusion-fixed for 3 min through the distal abdominal aorta with 100 mM sodium cacodylate/3% paraformaldehyde/2.5% glutaraldehyde/50 mM potassium oxalate. Tracheas were removed, incubated overnight in the perfusion buffer and then 3 days in 100 mM sodium cacodylate/1% OsO_4 /100 mM potassium ferricyanide before being embedded in Epon. Electron spectroscopic imaging of ultrathin sections was performed in the Zeiss EM 902 transmission electron microscope without further staining. To demonstrate precipitated Ca^{2+} salts, the L2.3 edge at $\Delta E=346$ eV was used.

Materials and statistical analysis All compounds (cyclopiazonic acid [CPA], ionomycin, ATP, okadaic acid, and Pak2 enzyme) were of highest available grade of purity and were from Sigma (Taufkirchen, Germany) or Merck (Darmstadt, Germany). All cell culture reagents were from GIBCO/Invitrogen (Karlsruhe, Germany). The following antibodies were used: mouse anti-hStim1 (Abcam 53551), goat anti-hSK4 (Santa Cruz sc-27081), rabbit anti-IP3R-I/II/III (Santa Cruz sc-28613), goat anti-hTRPC1 (Santa Cruz sc-15055), rabbit anti-h Na^+/K^+ ATPase (Upstate Biotechnology 21217), goat anti-hSERCA3 (Santa Cruz sc-8097). Goat antirabbit IgG-HRP (Acris R1364 HRP), donkey antigoat IgG-HRP (Santa Cruz sc-2020), and a mouse anti-His-Tag antibody (Qiagen) were used as secondary antibodies. Duplexes of 25-nucleotide RNAi were designed and synthesized by Invitrogen (Paisley, UK). siRNAs for hBest1, xBest2a, and xBest2b were: 5'-UGUCCUGUUGGCUGUGGAUGA GAU-3', 5'-AUCUGAAUACAUCUCAUCCACAGCC-3', 5'-GGCGGUGUAAGAUGUUUACUGGAU-3'. Student's *t* test (for paired or unpaired samples as appropriate) and analysis of variance were used for statistical analysis. $P<0.05$ was accepted as significant.

Results

Bestrophin 1 is localized in the ER The aim of the present study was to identify the mechanisms by which bestrophin 1 induces Ca^{2+} -dependent Cl^- conductance. Although bestrophin 1 is a Ca^{2+} -activated Cl^- channel that was found to be expressed in the plasma membrane [15, 28], other studies suggested that a significant portion of bestrophin 1, when overexpressed in HEK293 cells, is localized in the ER [26]. We examined hBest1 expressed endogenously in airway epithelial cells and found predominant expression in an intracellular compartment where it colocalizes with ER markers such as calreticulin, calnexin, or Stim1, the ER-

Ca^{2+} sensor [10, 47] (Fig. 1a). Each immunohistochemical staining was performed in triplicates. The dashed line indicates cell borders and makes clear that endogenous hBest1 in airway epithelial cells is essentially located intracellularly. This corresponds well with earlier findings, demonstrating intracellular expression of hBest1 in mouse-collecting duct cells [1]. Since hBest1 was found in the ER, we examined whether it is colocalized more intimately with typical ER proteins such as the Ca^{2+} -ATPase SERCA, IP_3 receptors (IP_3 -R), or Stim1. To that end, we performed additional experiments which indicated that hBest1 could be coimmunoprecipitated with Stim1 (Fig. 1b) but not with IP_3 -R, SERCA, or components of the store-operated Ca^{2+} influx pathway, such as TRPC1 (Supplement 1). Because hBest1 is localized in the ER, it may have a role in receptor-mediated intracellular Ca^{2+} signaling. In subsequent experiments, we, therefore, examined the effects of hBest1 on receptor-mediated Ca^{2+} signaling in HEK293 cells, which apparently do not express hBest1 [42]. However, we also found that HEK293 cells express small amounts of endogenous hBest1, as detected by RT-PCR and Western blotting. In addition, expression of endogenous hBest1 in HEK293 cells could be suppressed by hBest1-siRNA (Fig. 1c).

Bestrophin 1 is phosphorylated by Pak2 ER-localized hBest1 may affect Ca^{2+} release and reuptake and, therefore, control Ca^{2+} signaling. To understand the potential role of bestrophin 1 for intracellular Ca^{2+} signaling, we searched for additional binding partners. To that end, hBest1 was overexpressed in HEK293 cells, and coimmunoprecipitated proteins were separated by 2D-PAGE and subjected to MALDI-TOF analysis. We identified the p21-activated serine/threonine kinase Pak2 as a novel binding partner of hBest1. hBest1 carries a strong consensus sequence for Pak2 in the C terminus, and we, therefore, were able to in vitro phosphorylate hBest1 by hPak2 (Fig. 1d). In contrast, Pak2 phosphorylation was eliminated by mutating the responsible serine 358 to an alanine in the consensus sequence of hBest1 (hBest-S358A; Fig. 1d). Phosphorylation by Pak2 may change the activity of bestrophin 1 and may thereby affect intracellular Ca^{2+} signaling. An effect of Pak2 on intracellular Ca^{2+} signaling during T cell activation has been described recently [12].

Intracellular Ca^{2+} signaling is Cl^- dependent and is augmented by bestrophin 1 We measured intracellular Ca^{2+} concentrations ($[\text{Ca}^{2+}]_i$) in hBest1-transfected HEK293 cells, using Fura2 as a Ca^{2+} -sensitive dye. If bestrophin 1 affects intracellular Ca^{2+} signals, it is likely that it does so by operating as a Cl^- channel, and thus, the Cl^- concentration should determine the Ca^{2+} signal. We, therefore, examined ATP-induced Ca^{2+} signals in the absence and presence of extracellular Cl^- . Replacement of bath Cl^- by gluconate only

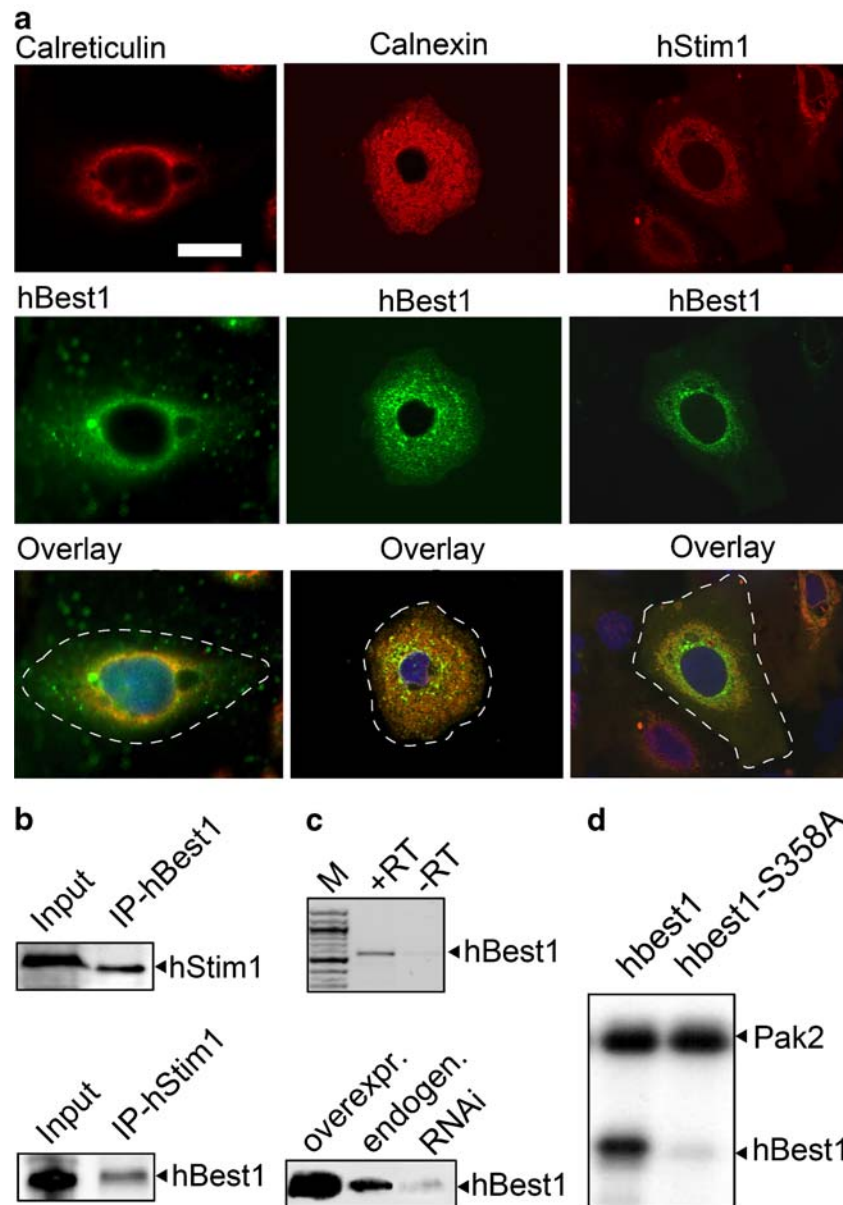


Fig. 1 Bestrophin 1 is localized in the ER. **a** Colocalization of hBest1 and the ER proteins calreticulin, calnexin (endogenous bestrophin 1, calreticulin, and calnexin, respectively, in human airway epithelial cells), and Stim1 (overexpression of bestrophin 1 and Stim1 in HEK293 cells). *Dashed line* indicates cell borders (*bar*=12 μ m). **b** Coimmunoprecipitation of hBest1 and hStim1 in lysates from HEK293 cells overexpressing both proteins. Equal amounts of protein

(20 μ g) were loaded, and experiments were performed at least in triplicates. **c** RT-PCR (*upper panel*) and Western blot analysis (*lower panel*) indicated the expression of endogenous hBest1 in HEK293 cells, which was suppressed by hBest1-RNAi. **d** In vitro phosphorylation of hBest1-C terminus by Pak2 and lack of Pak2 phosphorylation of hBest1-R218C

slightly reduced $[Ca^{2+}]_i$ but inhibited the Ca^{2+} peak and eliminated the Ca^{2+} plateau (Fig. 2a–c). This clearly points to a role of Cl^- in Ca^{2+} signaling. We, therefore, examined the influence of bestrophin 1 on ATP-induced Ca^{2+} signals. We found that the expression of hBest1 amplifies intracellular Ca^{2+} signals elicited by stimulation with ATP (10 μ M; Fig. 2d). Ca^{2+} peaks resembling ER store release were significantly augmented. Since previous work suggested that bestrophin 1 controls Ca^{2+} influx pathways, which may

indirectly affect Ca^{2+} peaks [33], we examined $[Ca^{2+}]_i$ increase upon inhibition of SERCA using CPA in the absence of extracellular Ca^{2+} . We found that, under these conditions, CPA-induced $[Ca^{2+}]_i$ increase was faster and more transient in cells overexpressing hBest1 (Fig. 2e).

Thus, the effects of bestrophin 1 on Ca^{2+} signals are similar in the presence or absence of extracellular Ca^{2+} , and therefore, it is unlikely that Ca^{2+} influx pathways contribute to the effects of bestrophin 1 on Ca^{2+} signaling observed

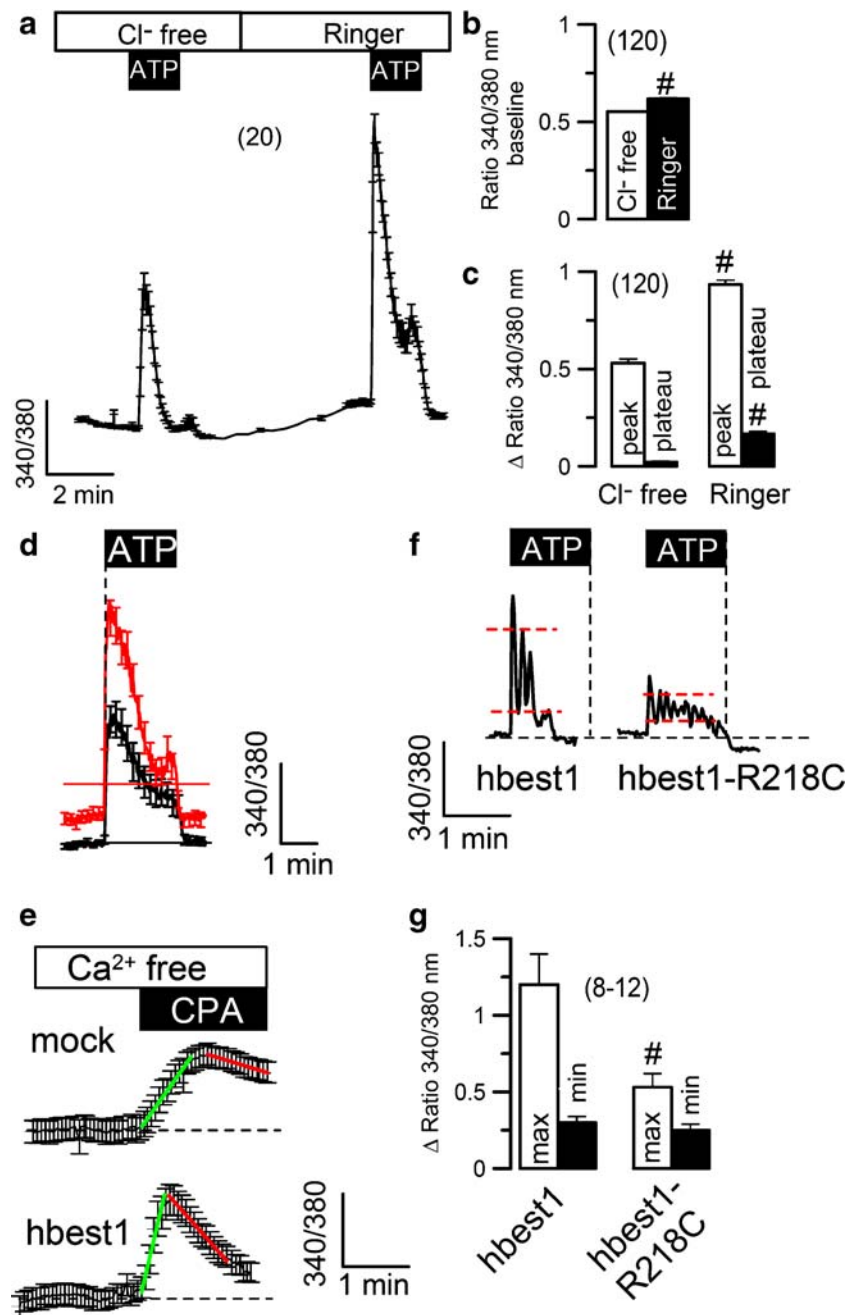


Fig. 2 Intracellular Ca^{2+} signaling is Cl^- dependent and is enhanced by bestrophin 1: **a** Summary curve (mean \pm SEM; $n=10$) for Ca^{2+} transients induced by ATP (10 μM) in HEK293 cells in the absence or presence of extracellular Cl^- . **b** Summary of the baseline Ca^{2+} concentrations indicates slightly enhanced baseline $[\text{Ca}^{2+}]_i$ in the presence of extracellular Cl^- . **c** Summary of peak and plateau Ca^{2+} increase indicates enhanced Ca^{2+} signaling in the presence of extracellular Cl^- . **d** Summary (mean \pm SEM; $n=10$) of Ca^{2+} transients induced by ATP (10 μM) in hBest1-expressing (red trace) or mock-transfected (black trace) HEK293 cells. **e** Emptying of ER- Ca^{2+} stores

by the SERCA-inhibitor CPA (10 μM) in the absence of extracellular Ca^{2+} in hBest1-expressing or mock-transfected HEK293 cells (mean \pm SEM; $n=16-27$). **f** ATP (100 μM)-induced oscillations of $[\text{Ca}^{2+}]_i$ detected by the Ca^{2+} probe G-CaMP2 fused to hBest1 (left trace) or hBest1-R218C (right trace), respectively. **g** Summary of upper (max) and lower (min) amplitudes of Ca^{2+} oscillations in cells expressing hBest1 or hBest1-R218C, respectively ($n=16-27$). Mean \pm SEM. The number sign indicates significant difference when compared to hBest1 or control (unpaired t test)

here. The results rather suggest that bestrophin 1 facilitates the release of Ca^{2+} from intracellular Ca^{2+} stores. We tried to measure cytosolic Ca^{2+} by a second independent method and in close proximity to the ER store and bestrophin 1.

We, therefore, fused the Ca^{2+} -sensitive protein G-CaMP2 [27] to hBest1 and to mutant hBest1-R218C, respectively. R218C eliminates ion channel function but is otherwise normally expressed, thereby causing an autosomal inherited

form of macular dystrophy of the retina [33]. Thus, overexpressed hBest1-R218C has a dominant negative effect on hBest1 expressed endogenously in HEK293 cells [38]. Expressing the hBest1-G-CaMP2 construct, we found that ATP is actually causing an oscillative $[Ca^{2+}]_i$ increase in HEK293 cells, rather than a typical peak and plateau response (Fig. 2f). Notably, the amplitudes for the Ca^{2+} oscillations (minimum–maximum) were large and short-lasting (number of oscillations = 4.1 ± 0.4 ; $n=8$) for hBest1-G-CaMP2, but were small (1.3 ± 0.3 ; $n=12$) and long-lasting (8.1 ± 0.5 ; $n=12$) for hBest1-R218C-G-CaMP2-expressing cells ($P < 0.05$; Fig. 2f, g). These results suggest that bestrophin 1 supports Ca^{2+} signaling by facilitating Ca^{2+} release from the ER store.

To be sure that we measure a true effect of bestrophin 1 on $[Ca^{2+}]_i$, we used a third method to measure $[Ca^{2+}]_i$ with the help of a membrane-bound Ca^{2+} dye (FFP-18) and assessed Ca^{2+} signals in intracellular membranous compartments. Using FFP-18, we found that ATP induced the typical peak/plateau response in control cells (Fig. 3a). In hBest1-overexpressing cells, the Ca^{2+} response was enhanced (1.3 ± 0.3 ; $n=17$) and more transient and showed Ca^{2+} oscillations (Fig. 3a). In contrast, the dominant negative mutant hBest1-R218C reduced the Ca^{2+} peak (0.5 ± 0.2 ; $n=24$, $P < 0.05$) and did not induce Ca^{2+} oscillations (Fig. 3a). Moreover, the rate of recovery from Ca^{2+} increase (Fig. 3, red lines) was 0.82 ± 0.1 (relative units per second; $n=12$) for control cells, was enhanced after expression of hBest1 (1.12 ± 0.2 ; $n=13$), but was significantly reduced by overexpression of hBest1-R218C (0.41 ± 0.08 ; $n=12$). Except for Ca^{2+} oscillations,

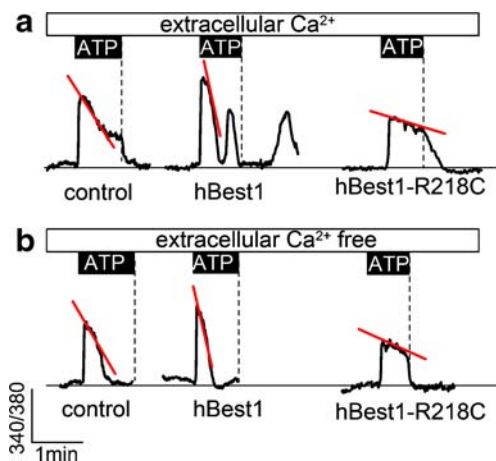


Fig. 3 Bestrophin 1 accelerates recovery from Ca^{2+} increase: ATP (100 μ M)-induced Ca^{2+} transients detected with the membrane-bound Ca^{2+} probe FFP-18 in the **a** absence (0 mM) or **b** presence (1.5 mM) of extracellular Ca^{2+} . Ca^{2+} transients were measured in (1) mock-transfected control cells, (2) hBest1-expressing cells, and (3) hBest1-R218C-expressing cells. hBest1 accelerates recovery from ATP-induced Ca^{2+} increase in both presence or absence of extracellular Ca^{2+} , while hBest1-R218C delays recovery from Ca^{2+} increase

which were not observed in the absence of extracellular Ca^{2+} , similar effects of bestrophin 1 and mutant hBest1-R218C were observed when Ca^{2+} was removed from the bath solution (Fig. 3b). Thus, bestrophin 1 enhances the Ca^{2+} peak and is causing a more transient Ca^{2+} response, which suggests a role for Ca^{2+} release from the store and reuptake back into the ER. Since bestrophin 1 has the function of a Ca^{2+} -activated Cl^- channel, it could act as a counterion channel to balance transient negative potentials generated by Ca^{2+} release and reuptake. It may thereby augment Ca^{2+} -dependent ion currents as described earlier [1, 4, 29].

Activation of TMEM16A Cl^- channels by bestrophin 1/Pak2

The data suggest that bestrophin 1 controls intracellular Ca^{2+} signaling and may, therefore, affect Ca^{2+} -dependent Cl^- channels in epithelial cells [4, 5, 26]. As in previous reports [26, 40] and also in the present study, we found that stimulation of hBest1-expressing HEK293 cells activated a whole-cell Cl^- current (Fig. 4a, b). Activation of Cl^- conductance is indicated by inhibition of the Cl^- current at low bath Cl^- concentration (30 mM; gray bars). This additional Cl^- conductance may be due to the fact that a fraction of overexpressed hBest1 reaches the cell membrane where it generates a Ca^{2+} -activated Cl^- current [26, 30, 40]. However, bestrophin 1 may also activate Ca^{2+} -dependent TMEM16A Cl^- channels, which we found to be expressed at low levels in HEK293 cells [2]. The kinase Pak2 phosphorylates bestrophin 1, and we found that coexpression of Pak2 together with bestrophin 1 largely augmented ATP-activated Cl^- currents. The effects of Pak2 and hBest1 on Ca^{2+} -dependent Cl^- channels in HEK293 cells were almost completely suppressed by hBest1-siRNA or by coexpression of the dominant negative mutant hBest1-R218C (Fig. 4a, b). Downregulation of hBest1 by siRNA was confirmed by Western blotting (Fig. 1c). These results indicate that the activation of Ca^{2+} -dependent Cl^- currents in HEK293 cells was controlled by bestrophin 1/Pak2. The recently identified TMEM16A is likely to resemble the molecular counterpart of ubiquitously expressed Ca^{2+} -activated Cl^- channels [11, 36, 44]. Overexpression of TMEM16A in our study produced large ATP-activated whole-cell Cl^- currents that were further augmented upon coexpression of hBest1 (Fig. 4c, d). In contrast, TMEM16A currents were reduced by coexpression of dominant negative hBest1-R218C. Since there is no indication for a direct interaction of bestrophin 1 with TMEM16A channels (Supplement 1), the most simple interpretation of these data is that bestrophin controls intracellular Ca^{2+} signals and thereby controls the activity of membrane-localized TMEM16A (Fig. 4d).

Endogenous Pak2 is important for the activation of Ca^{2+} -dependent Cl^- currents Human airway epithelial cell lines such as 16HBE14o $^-$ express both hBest1 and hTMEM16A

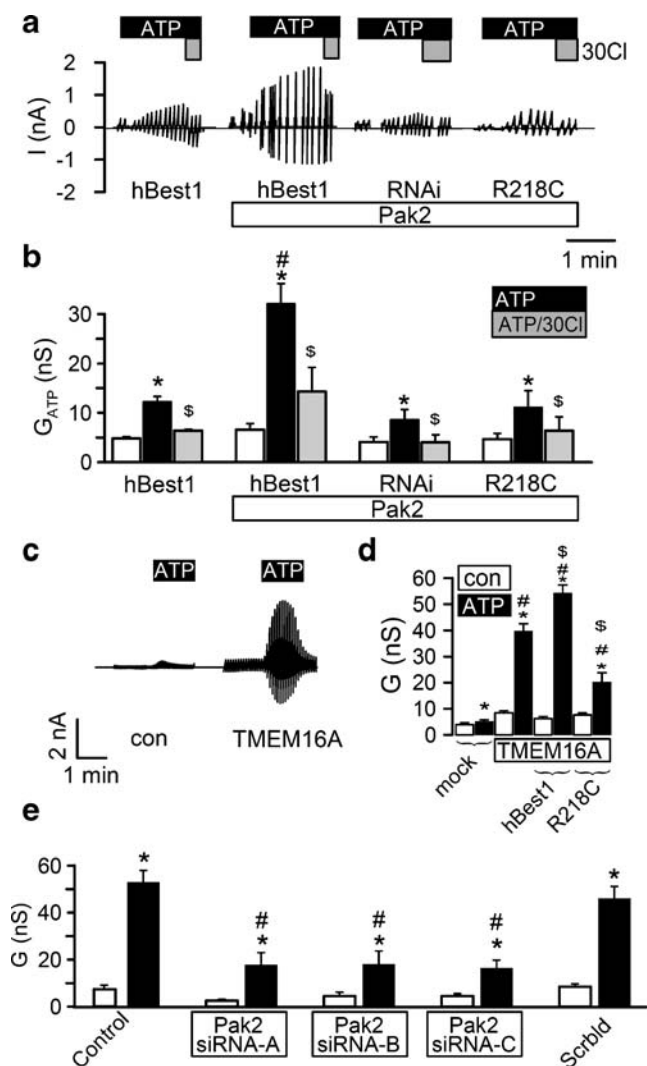


Fig. 4 Bestrophin 1/Pak2 activates TMEM16A Cl^- channels in mammalian cells: **a** ATP (100 μM)-activated whole-cell currents in hBest1-expressing HEK293 cells and in cells coexpressing Pak2/hBest1, Pak2/siRNA-hBest1, or Pak2/hBest1-R218C. Gray bars indicate partial removal of Cl^- (30 Cl^-) from the extracellular bath solution. **b** Whole-cell conductances under control conditions (white bars), after stimulation of ATP (black bars), and after partial removal of extracellular Cl^- (30 Cl^- ; gray bars; $n=9-15$). The dollar sign indicates significant inhibition of whole-cell conductance by 30 Cl^- (paired t test). **c** Activation of whole-cell currents by ATP in control HEK293 cells (left trace) and after the expression of hTMEM16A (right trace). **d** Summary of the whole-cell conductances in control cells (mock) and after expression of hTMEM16A, hTMEM16A/hBest1, or hTMEM16A/hBest1-R218C ($n=10-22$). The dollar sign indicates significant difference to TMEM16A (unpaired t test). **e** Endogenous whole-cell conductances in human bronchial epithelial cells before and after stimulation with ATP (100 μM). Three different batches of siRNA-Pak2 inhibited ATP-activated conductances ($n=11-38$). The asterisk indicates significant effect of ATP (paired t test). The number sign indicates significant difference when compared to hBest1 or control (unpaired t test)

endogenously [5, 11]. Here, we demonstrate again the importance of endogenous Pak2 for receptor-mediated and bestrophin 1-dependent activation of TMEM16A- Cl^- channels in 16HBE cells, by siRNA knockdown of Pak2. Three

independent batches of hPak2-siRNA significantly inhibited ATP activation of whole-cell Cl^- currents (Fig. 4e). Downregulation of Pak2 was confirmed by quantitative real-time RT-PCR (data not shown). Thus, bestrophin 1 and Pak2 are important regulators of Ca^{2+} -dependent ion channels in mammalian cells.

Pak2 activates Ca^{2+} -dependent TMEM16A Cl^- channels in *Xenopus* oocytes We examined the effects of Pak2 in *Xenopus* oocytes, which express large Ca^{2+} -activated Cl^- currents, endogenous xBest1 [31], and xTMEM16A Cl^- channels [36]. Ca^{2+} -dependent Cl^- channels were activated by ATP in P2Y₂-expressing *Xenopus* oocytes. Injection with active Pak2 enzyme largely enhanced ATP-induced, i.e., Ca^{2+} -activated, whole-cell currents (Fig. 5a, b). ATP-activated whole-cell Cl^- currents were suppressed by replacement of extracellular Cl^- by impermeable gluconate (5 Cl^- ; Fig. 5b). Notably, injection of Pak2 also augmented a delayed inward current activated by ATP. This current was inhibited by the removal of bath Na^+ and Ca^{2+} (Fig. 5a, c). Thus, Pak2 injection amplifies endogenous TMEM16A currents as well as a Ca^{2+} influx pathway, probably by enhancing Ca^{2+} release from ER- Ca^{2+} stores and activation of store-operated Ca^{2+} influx. Notably, whole-cell currents activated through direct increase in intracellular Ca^{2+} by ionomycin were not further activated by Pak2, indicating that Pak2 controls receptor-mediated activation of CaCC (Supplement 2B). In contrast to Pak2, injection of Pak1 did not augment Ca^{2+} -activated Cl^- currents or nonselective cation currents (Supplement 2C, D).

To further examine whether Pak2 acts through phosphorylation of xBest1 to activate Ca^{2+} -dependent Cl^- channels, we overexpressed the phosphorylation mutant hBest-S358A together with P2Y₂ receptors in *Xenopus* oocytes. While ATP activated a whole-cell conductance of $55.3 \pm 6.3 \mu\text{S}$ ($n=12$) in oocytes expressing P2Y₂ receptors only, ATP activated only $31.2 \pm 3.3 \mu\text{S}$ ($n=8$; $P \leq 0.05$) in oocytes coexpressing both P2Y₂ receptors and hBest-S358A. Moreover, after the injection of Pak2, ATP-induced conductance was $160 \pm 16.3 \mu\text{S}$ in P2Y₂-expressing oocytes but only $82 \pm 11.2 \mu\text{S}$ ($n=7$; $P \leq 0.05$) in cells coexpressing hBest-S358A. In additional experiments, we injected siRNA to knockdown endogenous *Xenopus* bestrophin (xBest2a, b). In both presence and absence of Pak2, ATP-induced but not ionomycin-induced whole-cell conductance was reduced in xBest2a, b siRNA-injected cells (data not shown). These experiments clearly suggest that Pak2 phosphorylates endogenous xBest2a, b and thereby amplifies ATP, i.e., Ca^{2+} -activated Cl^- currents.

A previous report indicated that bestrophin 1 interacts physically and functionally with protein phosphatase 2A (PP2A) [25]. We speculated that Pak2-phosphorylated Best1 is rapidly dephosphorylated and deactivated by PP2A [46]. In fact, in the presence of the PP2A-inhibitor

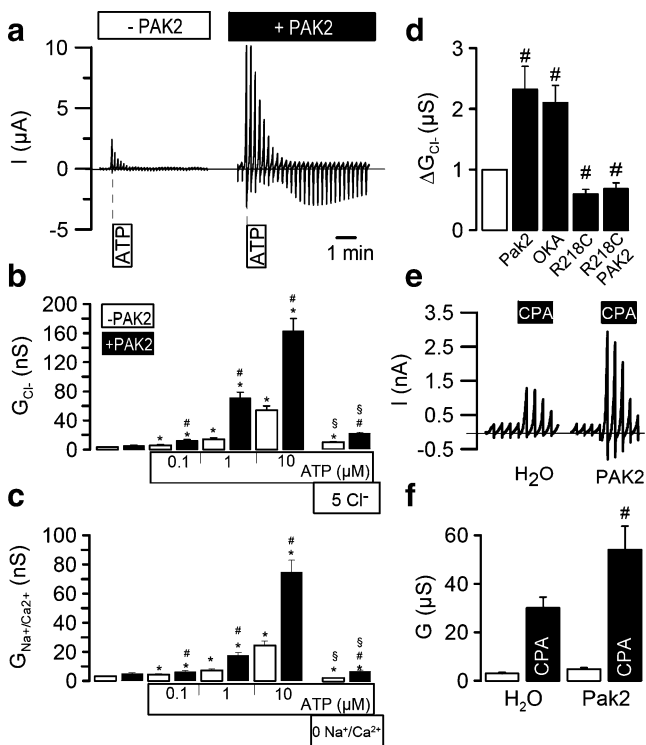


Fig. 5 Bestrophin 1/Pak2 activates Ca^{2+} -dependent Cl^- channels in *Xenopus* oocytes: **a** Whole-cell currents in *Xenopus* oocytes expressing P2Y_2 receptors (voltage clamped from -60 to $+40$ mV). ATP ($100 \mu\text{M}$) activated endogenous Ca^{2+} -dependent Cl^- currents. Injection of Pak2 ($2 \mu\text{g}/\mu\text{l}$) increased ATP-induced outward and inward currents. **b** Concentration-dependent activation of outward currents in the absence (open bars) or presence (black bars) of Pak2. Removal of extracellular Cl^- (5 mM) inhibited ATP-activated whole-cell currents. **c** Concentration-dependent activation of inward currents. Removal of extracellular Na^+ and Ca^{2+} ($0/0 \text{ mM}$) inhibited inward currents ($n=8-21$). **d** ATP-activated Cl^- conductances were augmented by injection of Pak2 ($2 \mu\text{g}/\mu\text{l}$) and exposure to okadaic acid (10 nM) but were inhibited by expression of hBest1-R218C ($n=16-38$). **e** Activation of Cl^- currents by inhibition of the SERCA pump with CPA ($10 \mu\text{M}$) in the absence and presence of Pak2. **f** Pak2 augmented CPA-activated Cl^- conductance ($n=9$). The asterisk indicates significant effect of ATP or ionomycin (paired t test). The number sign indicates significant difference when compared to absence of Pak2 (unpaired t test). The section sign indicates significant difference when compared to presence of Cl^- or $\text{Na}^+/\text{Ca}^{2+}$ (unpaired t test)

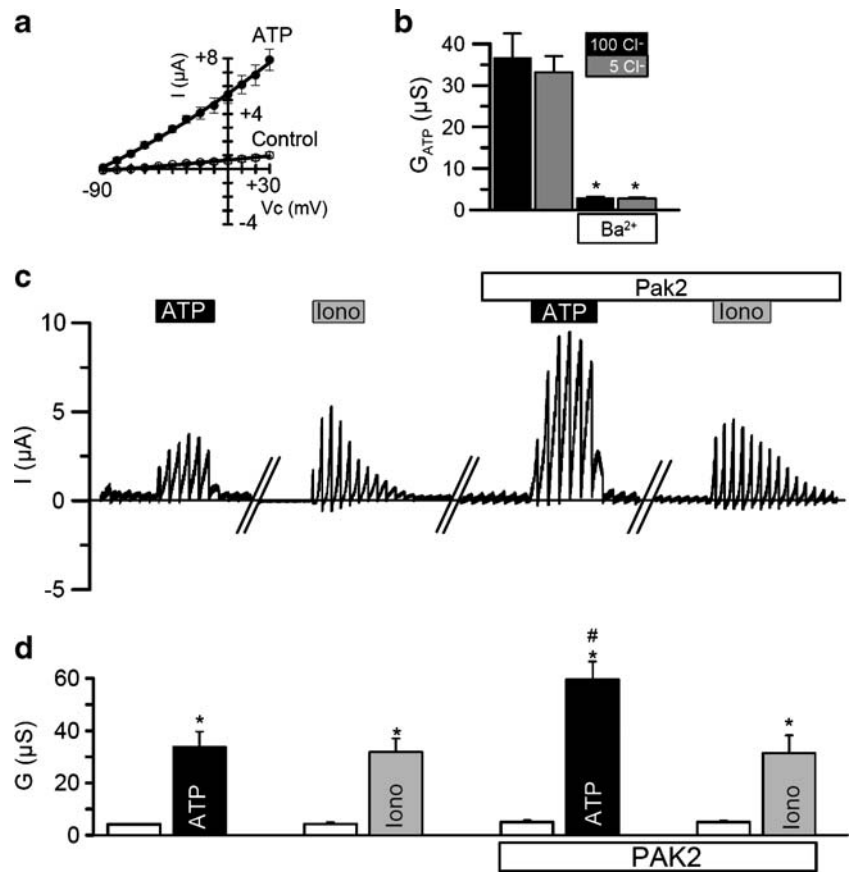
okadaic acid (10 nM), ATP-activated whole-cell conductance (G_{ATP}) was augmented to a similar magnitude as by injecting the Pak2 enzyme (Fig. 5d). In contrast, expression of dominant negative hBest-R218C reduced ATP-activated TMEM16A currents in *Xenopus* oocytes and completely abrogated the stimulating effect of Pak2, similar to that shown in Fig. 4a, b for mammalian cells (Fig. 5d). Noteworthy is that the activation of TMEM16A Cl^- currents in *Xenopus* oocytes through the depletion of ER- Ca^{2+} stores (inhibition of SERCA by CPA) was also augmented after injection of Pak2 (Fig. 5e, f). Therefore, similar effects of bestrophin 1 and Pak2 on Ca^{2+} -dependent Cl^- currents are observed in both mammalian cells and *Xenopus* oocytes. This phenomenon is not specific for

purinergic stimulation but was also observed for activation of whole-cell currents by endogenous receptors for lysophosphatidic acid (Supplement 2A).

Pak2 activates Ca^{2+} -dependent SK4 K^+ channels in *Xenopus* oocytes If bestrophin 1 and Pak2 activate plasma membrane-localized Cl^- channels by facilitating intracellular Ca^{2+} release, they should also be able to activate other Ca^{2+} -dependent ion channels such as the Ca^{2+} -activated K^+ channel SK4 [21]. To test this hypothesis, we expressed P2Y_2 receptors together with hSK4 in *Xenopus* oocytes. The membrane voltage of these oocytes was strongly hyperpolarized and was further hyperpolarized upon stimulation with ATP and activation of hSK4 (Fig. 6a). Activation of CaCC by ATP was negligible in hSK4-expressing oocytes, since the removal of extracellular Cl^- (5 Cl^-) did not compromise the ATP response, while 5 mM Ba^{2+} suppressed the activation of a whole-cell conductance by ATP (Fig. 6b). Moreover, the CaCC-inhibitor DIDS did not inhibit ATP-activated conductance ($-\text{DIDS}=18.3 \pm 2.1 \mu\text{S}$ vs $+\text{DIDS}=17.3 \pm 1.9 \mu\text{S}$; $n=17$), while the SK4-inhibitor TRAM-34 inhibited the effect of ATP significantly ($-\text{TRAM-34}=18.3 \pm 2.1 \mu\text{S}$ vs $+\text{TRAM-34}=6.43 \pm 1.5 \mu\text{S}$; $n=12$). We activated hSK4 K^+ currents in the absence or presence of Pak2, either through stimulation of purinergic receptors by ATP or directly by increasing $[\text{Ca}^{2+}]_i$ with ionomycin (Fig. 6c). Notably, receptor activation of hSK4 currents was augmented by Pak2, while activation through direct increase in $[\text{Ca}^{2+}]_i$ by ionomycin was not affected by Pak2 (Fig. 6c, d). Thus, not only Ca^{2+} -dependent TMEM16A channels are controlled by bestrophin 1/Pak2 but also Ca^{2+} -activated K^+ channels.

Bestrophin 1 is important for Ca^{2+} handling of the ER The present data suggest that bestrophin 1 is important for Ca^{2+} handling of the ER, probably by acting as a channel for the counterion Cl^- (Fig. 8). As shown earlier, airway epithelial cells from Best1 $^{-/-}$ mice display attenuated Ca^{2+} -activated Cl^- currents [4]. Since the lack of expression of Best1 Cl^- channels in the ER may cause structural changes, we decided to employ high-resolution electron microscopy to examine tracheal epithelial cells of mBest1 $^{-/-}$ mice. To our surprise, we detected bloated ER structures in cells of four different Best1 $^{-/-}$ mice (Fig. 7a, right panels, yellow arrows). These changes were not observed in airway cells of three control littermates (Fig. 7a, left panels). Moreover, using an oxalate-substituted fixative solution, we detected electron-dense Ca^{2+} precipitations in the ER of Best1 $^{-/-}$ mice (Fig. 7b, right panels). Similar structures were occasionally found in cells from Best1 $^{+/+}$ animals which, however, did not contain electron-dense Ca^{2+} precipitations (Fig. 7b, left panels). These findings are in striking similarity to the changes observed in mice that lack another counterion

Fig. 6 Pak2 activates Ca^{2+} -dependent SK4 K^+ channels in *Xenopus* oocytes: **a** *I/V* curves (mean \pm SEM) from SK4-expressing oocytes. Stimulation with ATP (10 μM) shifted the reversal potential to -90 mV ($n=12$). **b** Summary of ATP-activated whole-cell conductances in SK4-expressing *Xenopus* oocytes in the presence of high (100 mM) and low (5 mM) extracellular Cl^- concentration and in the absence or presence of Ba^{2+} (5 mM; $n=8$ for all). **c** Effect of Pak2 on K^+ currents activated by ATP (10 μM) or ionomycin (1 μM) in oocytes coexpressing P2Y_2 receptors and hSK4. **d** Pak2 augmented hSK4 whole-cell conductances, when activated by ATP but not by ionomycin ($n=19$ – 22). The asterisk indicates significant effect of ATP, ionomycin, or Ba^{2+} (paired *t* test). The number sign indicates significant difference when compared to the absence of Pak2 (unpaired *t* test)



channel in the sarcoplasmic reticulum (SR) of cardiomyocytes [45]. Taken together, we suggest that bestrophin 1 may operate as a counterion channel in the ER of epithelial cells to control Ca^{2+} filling and release. By doing so, it controls the activation of plasma membrane-localized Ca^{2+} -dependent Cl^- (TMEM16A) and K^+ (SK4) channels.

Discussion

Bestrophin 1 in the ER Bestrophin 1 is expressed in the basolateral membrane of the retinal pigment epithelium [24]. When overexpressed, bestrophins can be detected in the cell membrane [15, 28]; however, membrane expression is different for the four human and mouse paralogs. We found that mouse bestrophin 1 and human bestrophin 2 and 4 express well in membranes of HEK293 cells, while human bestrophin 1 and bestrophin 3 show little membrane localization [23, 26]. The present results confirm earlier findings that bestrophin 1 expressed endogenously in epithelial cells is localized in the ER [1, 23]. As demonstrated for mouse-collecting duct cells, expression of bestrophin 1 depends on cell density and proliferation which is likely to shape intracellular Ca^{2+} transients important for cell proliferation [1].

Bestrophin 1 controls intracellular Ca^{2+} signals The present data demonstrate that, in all experiments, the expression of bestrophin 1 significantly augmented the (peak) increase of intracellular Ca^{2+} , while inhibition of bestrophin 1 expression or overexpression of hBest1-R218C significantly reduced the peak response and delayed the time for recovery from Ca^{2+} increase. Bestrophin 1 is probably not the only ER-localized channel, and Cl^- is probably not the only ion that counterbalances charges during Ca^{2+} release and reuptake into the store, since cells lacking the expression of endogenous bestrophin 1 are able to generate peak/plateau Ca^{2+} signals. Notably, mice lacking bestrophin 1 expression survive well, although Ca^{2+} -activated Cl^- currents are reduced in airway epithelial cells of these animals [4]. These results suggest that bestrophin 1 is not essential for cell survival and function, but it modulates cellular properties such as proliferation and probably motility as well as Cl^- conductance [1].

Bestrophin 1 is controlled by Pak2 Bestrophin 1 was found to bind Pak2 and to be phosphorylated by Pak2. Pak2 is activated by autophosphorylation through binding of small G proteins such as Cdc42 and Rac1. It is transiently activated under cell stress and by phosphatidylinositol-3 kinase or tyrosine kinase or becomes permanently activated through cleavage by caspase-3 [18, 43]. Pak2 phosphorylation and translocation to the ER can induce either

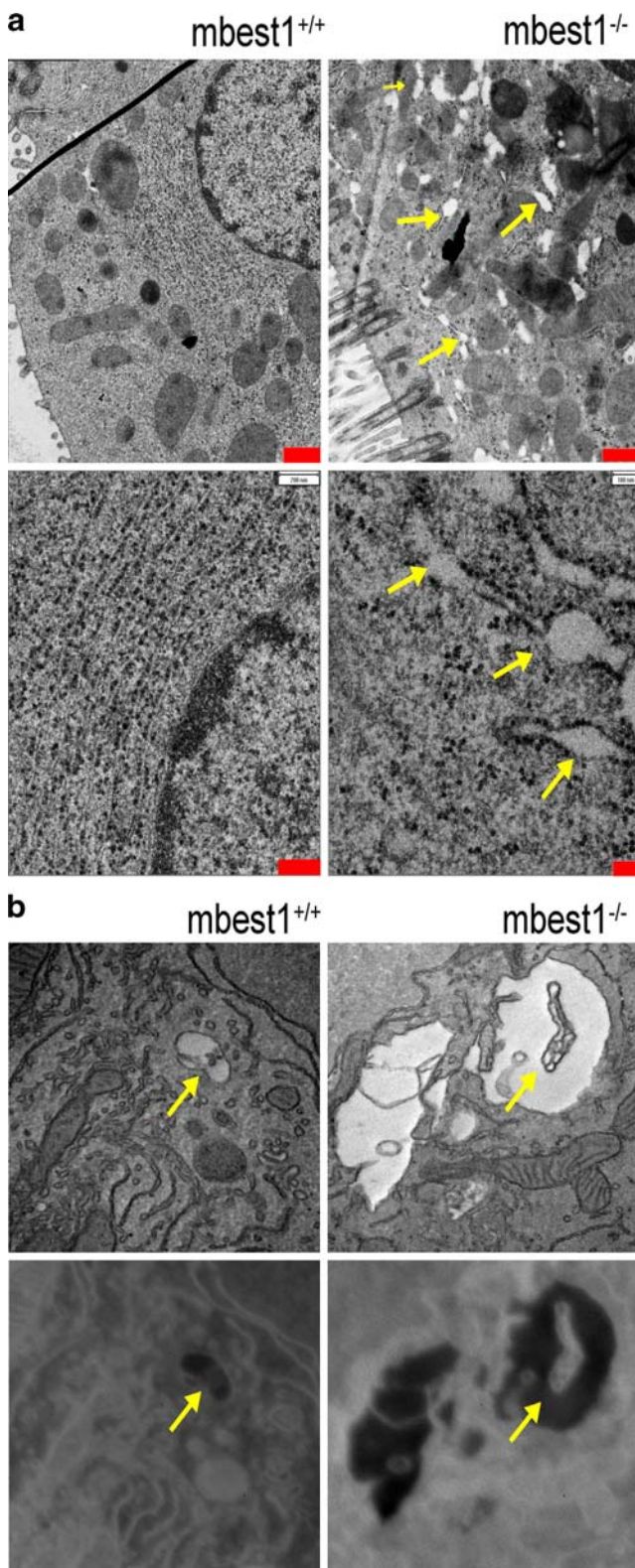


Fig. 7 Expanded ER in airway epithelial cells of mBest1 null mice: **a** Electron microscopy images of airway epithelial cells from Best1^{+/+} and Best1^{-/-} mice, at low (*upper panels*; red bar 600 nm) and high (*lower panels*; red bar 100 nm) magnification. EM images revealed swollen ER structures in epithelial cells of Best1^{-/-} mice (*right panels*; yellow arrows) that are not observed in cells from Best1^{+/+} animals (*left panels*). **b** Fixation with oxalate-containing solutions unmasked electron-dense Ca²⁺-oxalate deposits in the bloated ER of airway epithelial cells of Best1^{-/-} animals (*right upper panel*, yellow arrows). Occasionally, small precipitations were found in cells from Best1^{+/+} animals, which, however, were not identified as Ca²⁺ precipitations (*left upper panel*). To demonstrate precipitated Ca²⁺ salts, a special setting of the electron beam was used (L2.3 edge at ΔE=346 eV; *lower panels*). Bright color indicates precipitations with high Ca²⁺ concentration in the ER (in cells from Best1^{-/-} mice; yellow arrow, *right lower panel*). Precipitations in cells from Best1^{+/+} animals were not electron dense (yellow arrow; *left lower panel*)

activated by TGFβ1, and exposure to TGFβ1 has been shown recently to augment Ca²⁺-dependent Cl⁻ currents in collecting duct cells [44].

Bestrophin 1—a counterion channel It is well known that ion conductances affect intracellular Ca²⁺ signaling. For example, activation of voltage-dependent Ca²⁺ influx depends on membrane depolarization, which is controlled by the activity of K⁺ and Cl⁻ channels (discussed in [19]). In contrast, Ca²⁺ influx through store-operated Ca²⁺ channels is reduced with depolarization of the membrane voltage [14]. In addition, we found that not only Ca²⁺

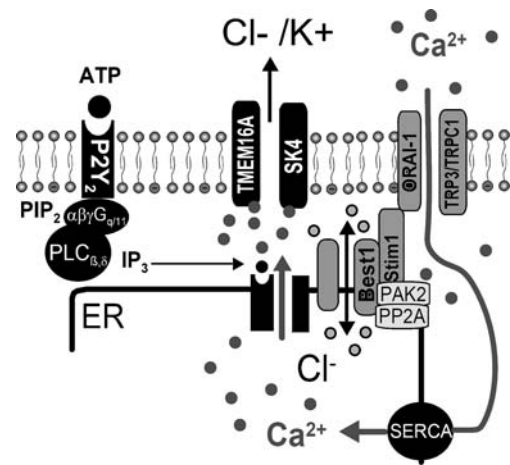


Fig. 8 Model for the role of bestrophin 1 as a counterion channel in the ER. ATP stimulation of purinergic receptors or other receptors coupling to phospholipase C (PLC) leads to increase of inositol triphosphate and release of Ca²⁺ from the endoplasmic reticulum (ER). ER-located bestrophin 1 acts as a counterion channel for Ca²⁺ release and reuptake (by the endoplasmic reticulum Ca²⁺ ATPase, SERCA) into the store by shuttling Cl⁻ ion over the ER membrane, thereby counteracting diffusion potentials arising from Ca²⁺ movement. Best1 binds to the Ca²⁺ sensor Stim1 (which binds to components of store-operated Ca²⁺ influx channels such as Orail1/Trp3/Trpc1), is phosphorylated by p21-activated protein kinase (Pak2), and is dephosphorylated by protein phosphatase 2A (PP2A). Thus, bestrophin 1 facilitates the activation of Ca²⁺-dependent TMEM16A Cl⁻ and SK4 K⁺ channels

proliferation or cytoskeleton/autophagy [18, 43]. Here, we report that Pak2 largely augmented receptor-mediated activation of Ca²⁺-dependent Cl⁻ and K⁺ channels in *Xenopus* oocytes. Notably, Pak2 is also known to be

influx but also Ca^{2+} release from the ER depends on the activity of plasma membrane ion channels and the membrane voltage (discussed in [34]).

The present data demonstrate that a Cl^- channel located in the ER controls intracellular Ca^{2+} signaling. The concept of a counterion channel in the ER to balance negative charges occurring through Ca^{2+} release and reuptake into the ER store has long been proposed [7]. In the SR, Cl^- channels play an essential role in excitation–contraction coupling, by balancing charge movement during calcium release and reuptake [13, 22]. This has also been well described in airway smooth muscle cells. SR-localized Cl^- channels in the SR membrane allow for neutralization of electrostatic charges that would otherwise build up during Ca^{2+} movement [16, 17]. Thus, SR-localized Cl^- channels support Ca^{2+} signaling and muscle contraction, and blocking these Cl^- channels might be an effective way in inhibiting airway smooth muscle hyper-responsiveness in asthma [16, 20]. Our present results suggest that bestrophin 1 is a counterion channel in the ER and thereby facilitates intracellular Ca^{2+} signaling in epithelial cells.

Also, cation channels have been proposed for counterion transport, such as the cation-selective channel TRIC [45]. TRIC knockout mice suffer from embryonic cardiac failure, and mutant cardiac myocytes show severe dysfunction in intracellular Ca^{2+} handling. The SR of these cells shows reduced K^+ permeability, and it was, therefore, concluded that TRIC channels act as counterion channels that function in synchronization with Ca^{2+} release from intracellular stores [45]. Electron microscopy revealed extensively swollen SR/ER structures in cardiomyocytes of TRIC knockout mice and showed frequent electron-dense Ca^{2+} -oxalate deposits in the bloated SR/ER. These changes are in striking similarity with our findings in airway epithelial cells of *Best1*^{-/-} mice. Notably, in the ER of pancreatic epithelial cells, the existence of an ATP-activated, DIDS-sensitive 64-kDa Cl^- channel has been described earlier [6]. These previous findings correspond well to the present data since 64 kDa is precisely the molecular weight of bestrophin 1 [23].

Bestrophin 1 and its role in disease The present data suggest that bestrophin 1 may operate as a counterion channel to control the activation of Ca^{2+} -dependent Cl^- (and K^+) channels (Fig. 8). As bestrophin 1 is upregulated during inflammation and tissue repair [1, 9], it may be in charge of the enhanced Ca^{2+} -dependent Cl^- conductance observed during inflammation and proliferation [1, 37]. Since Ca^{2+} oscillations are fundamental to cell proliferation [8], it will be interesting to learn whether overexpression of bestrophin 1 in cancer cells induces malignancy by affecting intracellular Ca^{2+} oscillations [37]. Moreover, enhanced Ca^{2+} -dependent Cl^- secretion as observed in cystic fibrosis has

been shown to be caused by an expansion of apical ER- Ca^{2+} stores [32]. Our own preliminary results show enhanced expression of bestrophin 1 in airway epithelial cells under proinflammatory conditions such as cystic fibrosis and asthma ([35] and unpublished findings from the author's laboratory). Thus, bestrophin 1 may play an unexpected role in a variety of diseases, apart from its central role in Best vitelliform macular dystrophy [39].

Acknowledgments This study was supported by the grants DFG SFB699 A6/A7, DFG KU 756/8-2, and Else Kröner-Fresenius-Stiftung P36/05//A44/05. We are grateful for the technical expertise of Caio Toledo, Christine Meese, Karin Schadendorf, Helga Schmidt, and Uwe de Vries in performing the ultrastructural analysis. The Ca^{2+} -sensitive GFP protein G-CaMP2 was kindly provided by Dr. J. Nakai, Wako City Saitama, Japan. We gratefully acknowledge the supply of the *vmd2*^{-/-} mice by MERCK Research Laboratories (770 Summeytown Pike, West Point, PA, USA).

References

- AlDehni F, Spitzner M, Martins JR, Barro Soria R, Schreiber R, Kunzelmann K (2009) Role of bestrophin for proliferation and in epithelial to mesenchymal transition. *J Am Soc Nephrol* 20:1556–1564
- Almaza J, Tian Y, AlDehni F, Ousingsawat J, Kongsuphol P, Rock JR, Harfe BD, Schreiber M, Kunzelmann K (2009) TMEM16 proteins produce volume regulated chloride currents that are reduced in mice lacking TMEM16A. *J Biol Chem*. doi:10.1074/jbc.M109.010074
- Bachhuber T, König J, Voelcker T, Mürle B, Schreiber R, Kunzelmann K (2005) Chloride interference with the epithelial Na^+ channel ENaC. *J Biol Chem* 280:31587–31594
- Barro Soria R, Schreiber R, Kunzelmann K (2008) Bestrophin 1 and 2 are components of the Ca^{2+} activated Cl^- conductance in mouse airways. *Biochim Biophys Acta* 1783:1993–2000
- Barro Soria R, Spitzner M, Schreiber R, Kunzelmann K (2006) Bestrophin 1 enables Ca^{2+} activated Cl^- conductance in epithelia. *J Biol Chem* 281:17460–17467
- Begault B, Anagnostopoulos T, Edelman A (1993) ATP-regulated chloride conductance in endoplasmic reticulum (ER)-enriched pig pancreas microsomes. *Biochim Biophys Acta* 1152:319–327
- Berridge MJ (2002) The endoplasmic reticulum: a multifunctional signaling organelle. *Cell Calcium* 32:235–249
- Berridge MJ, Irvine RF (1989) Inositol phosphates and cell signalling. *Nature* 341:197–205
- Boudes M, Sar C, Menigoz A, Hilaire C, Pequignot MO, Kozlenkov A, Marmorstein AD, Carroll P, Valmier J, Scamps F (2009) Best1 is a gene regulated by nerve injury and required for Ca^{2+} -activated Cl^- current expression in axotomized sensory neurons. *J Neurosci* 29:10063–10071
- Brandman O, Liou J, Park WS, Meyer T (2007) STIM2 is a feedback regulator that stabilizes basal cytosolic and endoplasmic reticulum Ca^{2+} levels. *Cell* 131:1327–1339
- Caputo A, Caci E, Ferrera L, Pedemonte N, Barsanti C, Sondo E, Pfeiffer U, Ravazzolo R, Zegarra-Moran O, Galletta LJ (2008) TMEM16A, a membrane protein associated with calcium-dependent chloride channel activity. *Science* 322:590–594
- Chu PC, Wu J, Liao XC, Pardo J, Zhao H, Li C, Mendenhall MK, Pali E, Shen M, Yu S, Taylor VC, Aversa G, Molineaux S, Payan DG, Masuda ES (2004) A novel role for p21-activated protein kinase 2 in T cell activation. *J Immunol* 172:7324–7334

13. Coonan JR, Lamb GD (1998) Effect of chloride on Ca^{2+} release from the sarcoplasmic reticulum of mechanically skinned skeletal muscle fibres. *Pflugers Arch* 435:720–730
14. Fischer KG, Leipziger J, Rubini-Illes P, Nitschke R, Greger R (1996) Attenuation of stimulated Ca^{2+} influx in colonic epithelial (HT₂₉) cells by cAMP. *Pflugers Arch* 432:735–740
15. Hartzell HC (2008) Molecular physiology of bestrophins: multi-functional membrane proteins linked to best disease and other retinopathies. *Physiol Rev* 88:639–672
16. Hirota S, Helli P, Janssen LJ (2007) Ionic mechanisms and Ca^{2+} handling in airway smooth muscle. *Eur Respir J* 30:114–133
17. Hirota S, Trimble N, Pertens E, Janssen LJ (2006) Intracellular Cl^- fluxes play a novel role in Ca^{2+} handling in airway smooth muscle. *Am J Physiol Lung Cell Mol Physiol* 290:L1146–L1153
18. Huang Z, Ling J, Traugh JA (2003) Localization of p21-activated protein kinase gamma-PAK/Pak2 in the endoplasmic reticulum is required for induction of cytotaxis. *J Biol Chem* 278:13101–13109
19. Janssen LJ (2002) Ionic mechanisms and Ca^{2+} regulation in airway smooth muscle contraction: do the data contradict dogma? *Am J Physiol Lung Cell Mol Physiol* 282:L1161–L1178
20. Janssen LJ (2009) Asthma therapy: how far have we come, why did we fail and where should we go next? *Eur Respir J* 33:11–20
21. Joiner WJ, Wang LY, Tang MD, Kaczmarek LK (1997) hSK4, a member of a novel subfamily of calcium-activated potassium channels. *Proc Natl Acad Sci USA* 94:11013–11018
22. Kourie JI (1997) ATP-sensitive voltage- and calcium-dependent chloride channels in sarcoplasmic reticulum vesicles from rabbit skeletal muscle. *J Membr Biol* 157:39–51
23. Kunzelmann K, Milenkovic VM, Spitzner M, Barro Soria R, Schreiber R (2007) Calcium dependent chloride conductance in epithelia: Is there a contribution by Bestrophin? *Pflugers Arch* 454:879–889
24. Marmorstein AD, Marmorstein LY, Rayborn M, Wang X, Hollyfield JG, Petrukhin K (2000) Bestrophin, the product of the Best vitelliform macular dystrophy gene (VMD2), localizes to the basolateral plasma membrane of the retinal pigment epithelium. *Proc Natl Acad Sci USA* 97:12758–12763
25. Marmorstein LY, McLaughlin PJ, Stanton JB, Yan L, Crabb JW, Marmorstein AD (2002) Bestrophin interacts physically and functionally with protein phosphatase 2A. *J Biol Chem* 277(34):30591–30597
26. Milenkovic VM, Schreiber R, Barro Soria R, AlDehni F, Kunzelmann K (2009) Functional assembly and purinergic activation of bestrophins. *Pflugers Arch* 458:431–441
27. Nakai J, Ohkura M, Imoto K (2001) A high signal-to-noise Ca^{2+} probe composed of a single green fluorescent protein. *Nat Biotechnol* 19:137–141
28. O'Driscoll KE, Leblanc N, Hatton WJ, Britton FC (2009) Functional properties of murine bestrophin 1 channel. *Biochem Biophys Res Commun* 384:476–481
29. Park KS, Jeon SH, Oh JW, Choi KY (2004) p21Cip/WAF1 activation is an important factor for the ERK pathway dependent anti-proliferation of colorectal cancer cells. *Exp Mol Med* 36:557–562
30. Qu Z, Fischmeister R, Hartzell HC (2004) Mouse bestrophin-2 is a bona fide Cl^- channel: identification of a residue important in anion binding and conduction. *J Gen Physiol* 123:327–340
31. Qu Z, Wei RW, Mann W, Hartzell HC (2003) Two bestrophins cloned from *Xenopus laevis* oocytes express Ca-activated Cl^- currents. *J Biol Chem* 278:49563–49572
32. Ribeiro CM, Paradiso AM, Carew MA, Shears SB, Boucher RC (2005) Cystic fibrosis airway epithelial Ca^{2+}_i signaling. The mechanism for the larger agonist-mediated Ca^{2+}_i signals in human cystic fibrosis airway epithelia. *J Biol Chem* 280:10202–10209
33. Rosenthal R, Bakall B, Kinnick T, Peachey N, Wimmers S, Wadelius C, Marmorstein AD, Strauss O (2006) Expression of bestrophin-1, the product of the VMD2 gene, modulates voltage-dependent Ca^{2+} channels in retinal pigment epithelial cells. *FASEB J* 20:178–180
34. Schreiber R (2005) Ca^{2+} signaling, intracellular pH and cell volume in cell proliferation. *J Membr Biol* 205:129–137
35. Schreiber R, Castrop H, Kunzelmann K (2008) Allergen induced airway hyperresponsiveness is absent in ecto-5'-nucleotidase (CD73) deficient mice. *Pflugers Arch* 457:431–440
36. Schroeder BC, Cheng T, Jan YN, Jan LY (2008) Expression cloning of TMEM16A as a calcium-activated chloride channel subunit. *Cell* 134:1019–1029
37. Spitzner M, Martins JR, Barro Soria R, Ousingsawat J, Scheidt K, Schreiber R, Kunzelmann K (2008) Eag1 and bestrophin 1 are upregulated in fast growing colonic cancer cells. *J Biol Chem* 283:7421–7428
38. Stanton JB, Goldberg AF, Hoppe G, Marmorstein LY, Marmorstein AD (2006) Hydrodynamic properties of porcine bestrophin-1 in Triton X-100. *Biochim Biophys Acta* 1758:241–247
39. Strauss O (2005) The retinal pigment epithelium in visual function. *Physiol Rev* 85:845–881
40. Sun H, Tsunenari T, Yau KW, Nathans J (2001) The vitelliform macular dystrophy protein defines a new family of chloride channels. *Proc Natl Acad Sci USA* 99:4008–4013
41. Takeshima H, Komazaki S, Hirose K, Nishi M, Noda T, Iino M (1998) Embryonic lethality and abnormal cardiac myocytes in mice lacking ryanodine receptor type 2. *EMBO J* 17:3309–3316
42. Tsunenari T, Sun H, Williams J, Cahill H, Smallwood P, Yau KW, Nathans J (2003) Structure–function analysis of the bestrophin family of anion channels. *J Biol Chem* 278:41114–41125
43. Wilkes MC, Murphy SJ, Garamszegi N, Leof EB (2003) Cell-type-specific activation of PAK2 by transforming growth factor beta independent of Smad2 and Smad3. *Mol Cell Biol* 23:8878–8889
44. Yang YD, Cho H, Koo JY, Tak MH, Cho Y, Shim WS, Park SP, Lee J, Lee B, Kim BM, Raouf R, Shin YK, Oh U (2008) TMEM16A confers receptor-activated calcium-dependent chloride conductance. *Nature* 455:1210–1215
45. Yazawa M, Ferrante C, Feng J, Mio K, Ogura T, Zhang M, Lin PH, Pan Z, Komazaki S, Kato K, Nishi M, Zhao X, Weisleder N, Sato C, Ma J, Takeshima H (2007) TRIC channels are essential for Ca^{2+} handling in intracellular stores. *Nature* 448:78–82
46. Zhan Q, Ge Q, Ohira T, Van Dyke T, Badwey JA (2003) p21-activated kinase 2 in neutrophils can be regulated by phosphorylation at multiple sites and by a variety of protein phosphatases. *J Immunol* 171:3785–3793
47. Zhang SL, Yu Y, Roos J, Kozak JA, Deerinck TJ, Ellisman MH, Stauderman KA, Cahalan MD (2005) STIM1 is a Ca^{2+} sensor that activates CRAC channels and migrates from the Ca^{2+} store to the plasma membrane. *Nature* 437:902–905